Research Article

MicroRNA Expression in Cutaneous Lupus: A New Window to Understand Its Pathogenesis

Silvia Méndez-Flores,[1] **Janette Furuzawa-Carballeda** [iD],[2] **Gabriela Hernández-Molina** [iD],[2] **Gustavo Ramírez-Martinez,**[3,4] **Nora E. Regino-Zamarripa,**[3] **Blanca Ortiz-Quintero,**[5] **Luis Jiménez-Alvarez,**[3] **Alfredo Cruz-Lagunas** [iD],[3] **and Joaquín Zúñiga** [iD][3,4]

[1]Department of Dermatology, Instituto Nacional de Ciencias Médicas y Nutrición Salvador Zubirán, Mexico City, Mexico
[2]Department of Immunology and Rheumatology, Instituto Nacional de Ciencias Médicas y Nutrición Salvador Zubirán, Mexico City, Mexico
[3]Laboratory of Immunobiology and Genetics, Instituto Nacional de Enfermedades Respiratorias Ismael Cosío Villegas, Mexico City, Mexico
[4]Tecnologico de Monterrey, Escuela de Medicina y Ciencias de la Salud, Mexico City, Mexico
[5]Department of Biochemistry, Instituto Nacional de Enfermedades Respiratorias Ismael Cosío Villegas, Mexico City, Mexico

Correspondence should be addressed to Janette Furuzawa-Carballeda; jfuruzawa@gmail.com
and Joaquín Zúñiga; joazu@yahoo.com

Background. The role of miRNAs in the pathogenesis of cutaneous lupus has not been studied. *Objective*. It was to assess the levels of a selected panel of circulating miRNAs that could be involved in the regulation of the immune response, inflammation, and fibrosis in cutaneous lupus. *Methods*. It was a cross-sectional study. We included 22 patients with subacute (SCLE) and 20 with discoid (DLE) lesions, and 19 healthy donors (HD). qRT-PCR for miRNA analysis, flow cytometry in peripheral blood, and skin immunohistochemistry were performed to determine the distribution of CD4 T cells and regulatory cells and their correlation with circulating miRNAs. *Results*. miR-150, miR-1246, miR-21, miR-23b, and miR-146 levels were downregulated in SCLE *vs.* HD. miR-150, miR-1246, and miR-21 levels were downregulated in DLE *vs.* HD. Peripheral $CD4^+/CD25^-/IL-4^+$ cells and $CD4^+/CD25^{hi}/Foxp3^+$ were negatively associated with miR-23b, and $CD4^+/CD25^-/IFN-\gamma^+$ with miR-1246 in SCLE, whereas $CD123^+/CD196^+/IDO^+$ cells were positively associated with miR-150 in DLE. In the tissue, $CD4^+/IL-4^+$ and $CD20^+/IL-10^+$ cells were positively associated with miR-21 and $CD4^+/IFN-\gamma^+$ with miR-31 in SCLE, whereas $CD4^+/IL-4^+$ cells were positively associated with miR-150, and $CD20^+/IL-10^+$ cells with miR-1246 and miR-146a in DLE. In the SCLE, lower miR-150 levels were correlated with higher CLASI scores. The KEGG pathway enrichment analysis revealed that cell cycle regulation pathways, p53, TGF-β, thyroid hormone, and cancer signaling pathways were shared between miR-21, miR-31, miR-23b, miR-146a, miR-1246, and miR-150. *Conclusions*. A downregulation of miR-150, miR-1246, and miR-21 in both CLE varieties *vs.* HD was determined.

1. Introduction

Cutaneous lupus erythematosus (CLE) is an autoimmune condition that comprehends a wide range of dermatological manifestations and clinical phenotypes. Its pathogenesis is multifactorial and involves genetic predisposition, environmental factors (ultraviolet light B), and abnormalities in the innate and adaptive immune response. In this context, the participation of some proinflammatory cytokines such as IFN-α, IL-1, IL-6, and TNF-α has been also recognized [1, 2]. Histological analysis of CLE skin is characterized by a dense periadnexal and perivascular lymphocytic infiltrate, mainly composed by $CD4^+$ helper T cells, $CD8^+$ cytotoxic T cells, B cells, and macrophages [1]. Moreover, the

participation of Th17 and Th22 CD4$^+$ T cells as well as regulatory T cells has been recently described [3, 4]. In addition, the activation of pathways via pattern recognition receptor (PRR) signaling, Janus kinase- (JAK-) signal transducer and activator of transcription (STAT) signaling, and nuclear factor-κB (NF-κB) signaling also have a role in CLE [5].

Recent studies have revealed the potential contribution of microRNAs (miRNAs) in diverse autoimmune diseases [6]. miRNAs are a class of small noncoding RNAs that modulate gene expression at the posttranscriptional level. They bind to the target messenger RNA, leading either to translational repression or to degradation. miRNAs regulate diverse physiologic processes, and their dysregulation can result in aberrant responses including impaired immune function [6–8].

For instance, in systemic lupus erythematosus (SLE), miRNA expression has been detected in the plasma [9], serum [10], urine, and peripheral blood mononuclear cells (PBMCs) [11]. Diverse miRNA patterns have been associated with a certain feature such as renal involvement (miR-146a), childhood onset (miR-516a-3p, miR-629, and miR-525-5p), and overall disease activity (miR-21 and miR-146a) [9–11] and recently, in discoid lupus (DLE) (miR-31 and miR-485-3p) [12]. Indeed, a study suggested miR-29b as a potential SLE diagnostic biomarker. The authors in that study, using a ROC curve analysis, showed an AUC of 0.75 (95% CI 0.64–0.86) for diagnosing SLE [13].

On the other hand, research focused on understanding the role of miRNAs in the regulation of signaling pathways may lead to develop new biomarkers and new therapeutic approach. In this sense, circulating miR-29b was also proposed as a biomarker to estimate lupus activity as it positively correlated with the SLEDAI score and anti-dsDNA titer and inversely correlated with complement C3 level and clinical response after treatment [13].

Herein, we hypothesized that the expression of a circulating miRNA signature might distinguish CLE patients and its subtypes. Therefore, our main objective was to evaluate the circulating levels of a selected panel of miRNAs based on their possible participation in the regulation of the immune response, inflammation, and fibrosis among patients with CLE. Specifically, we evaluated the following miRNAs: miR-29 family that regulates T cell polarization [14]; miR-150 involved in B and Th17 cell differentiation and TGF-β signaling [15]; miR-23b related to IL-17, TNF-α, and IL-1β expression [16]; miR-1246 which is associated to B cell activation [17]; miR-21 inked with Th2 and Th17 differentiation and Foxp3$^+$ expression [18]; miR-31 that regulates Treg cells, NF-κB activation, and fibrosis [19]; miR-146 that appears to downregulate NF-κB and TLR/MyD88 proinflammatory signal pathways [20, 21]; miR-155 that contributes to Th1 and Th17 differentiation [22]; miR-485 that participates in Th2 differentiation [12]; and miR-197 that allows the IL-22 responses [23]. Moreover, we also correlated these serum miRNAs with T, B, and regulatory cell subpopulations in the skin tissue and peripheral blood as well as with the CLASI activity score. Finally, we elucidated their possible participation in CLE pathogenesis applying bioinformatics.

2. Materials and Methods

2.1. Patients.
This was a cross-sectional study conducted in a tertiary care center. We included 42 consecutive patients with CLE: 22 with subacute cutaneous lupus (SCLE) and 20 with DLE. To be eligible, patients also had to meet the classification criteria for SLE according to the ACR criteria [24] and to have an active lupus-specific lesion compatible with SCLE or DLE. The diagnosis of CLE was established in consensus by a rheumatologist and a dermatologist, as well as by biopsy. In addition, patients should not be under topical treatment including steroids within the last 6 weeks. However, patients could maintain their basal oral steroids and immunosuppressants. Patients were excluded if they had any concomitant cutaneous lesion not attributed to lupus or an overlap autoimmune condition.

We included 19 healthy donors (HD) as controls. The control group did not have any autoimmune disease and/or concurrent infection and did not receive prednisone or immunosuppressants.

We measured the CLASI, a validated index to quantify disease severity [25]. As this instrument measures both activity and damage, for the present study, we only used the activity domain that ranges from 0 to 70 (higher scores are indicative of more severity).

In addition, patients' clinical records were carefully reviewed according to a preestablished protocol to collect demographics as well as other clinical and serologic features.

2.2. Skin Samples.
Skin punch biopsies (4 mm diameter) were performed, fixed in formalin, and evaluated with hematoxylin-eosin staining for the assessment of classic histologic cutaneous lupus features. Then, the rest of the specimen was stored for immunohistochemistry. Microscopic review was performed in a blinded manner to the diagnosis by one blinded observer.

Overall, most of the cutaneous lupus biopsies corresponded to photoexposed areas localized at the arms, thorax, or scalp. Control tissue biopsies were also taken from photoexposed areas and, if possible, from the same anatomical zone.

2.3. Immunohistochemistry.
We followed the methods of Méndez-Flores et al. [26]. Briefly, IL-22-expressing cells were determined in 4 μm thick sections of tissue. After deparaffinization and demasking of antigens, tissues were blocked with 3% H$_2$O$_2$. Then, nonspecific background staining was avoided with the IHC background blocker (Enzo Life Sciences). Tissues were incubated with goat polyclonal anti-human IL-22 antibody (Santa Cruz Biotechnology, Santa Cruz, CA, USA) at 10 μg/ml. Binding was identified with biotinylated donkey anti-goat IgG antibody (ABC Staining System; Santa Cruz Biotechnology). Slides were incubated with horseradish peroxidase- (HRP-) streptavidin, followed by incubation with the peroxidase substrate 3,3-diaminobenzidine (DAB) (Sigma-Aldrich) for 10 min. The sections were counterstained with hematoxylin. Negative control staining was performed with normal human serum diluted 1 : 100, instead of primary antibody, and the IHC universal negative

control reagent (IHC universal negative control reagent, Enzo Life Sciences). The reactive blank was incubated with phosphate buffer saline-egg albumin (Sigma-Aldrich) instead of the primary antibody. Both controls excluded nonspecific staining or endogenous enzymatic activities [26]. Spleen and ganglion samples were used as a positive control (Figure S1).

2.4. Double-Staining Procedure.

We followed the methods of Méndez-Flores et al. [26]. To determine the subpopulation of CD4$^+$/IL-17A$^+$–, CD4$^+$/IL-4$^+$–, CD4$^+$/IFN-γ^+-expressing T cells, CD25$^+$/Foxp3$^+$ regulatory T cells, CD20$^+$/IL-10$^+$-producing B cells, and CD123$^+$/IDO$^+$ pDC cell subpopulations, a simultaneous detection was performed (MultiView (mouse-HRP/rabbit-AP) Enzo Life Sciences). After deparaffinization and demasking of antigens with the antigen retrieval reagent (Enzo Life Sciences), tissues were blocked with 3% H$_2$O$_2$. The procedure is a sequential double staining where the first antigen (normal serum as negative control, rabbit polyclonal anti-IL-17A, anti-IL-4, anti-IFN-γ, anti-IDO IgG antibody, or mouse monoclonal anti-IL-10 or anti-Foxp3 IgG$_1$ antibody (Santa Cruz Biotechnology) at 10 μg/ml) was visualized using horseradish peroxidase (HRP)/3$'$3$'$-diaminobenzidine (DAB) and the second antigen (normal serum as negative control or second primary rabbit polyclonal anti-CD20, anti-CD25 IgG antibody or mouse monoclonal anti-CD4, anti-IgG$_1$ antibody (Santa Cruz Biotechnology), or anti-CD123 IgG antibody (Abcam pcl, CA, UK) at 10 μg/ml) was visualized using alkaline phosphatase (AP)/Permanent Red. Tissues were counterstained with Mayer's hematoxylin and mounted in aqueous mounting medium. Cytokine-expressing cells as well as double positive cells were assessed by estimating the number of positively staining cells in two fields (X320) and were reported as the percentage of immunoreactive cells of the inflammatory infiltrates located at the epidermis and dermis. Results are expressed as the mean ± standard error of the mean (SEM) of cells quantified by the program Image Pro Plus version 5·1·1 [26].

2.5. Peripheral Blood Samples.

A venous blood sample was drawn from each subject to perform flow cytometry analysis and RNA isolation.

2.6. Flow Cytometry.

Peripheral blood mononuclear cells (PBMCs) were obtained by gradient centrifugation on Lymphoprep (Axis-Shield PoC AS, Oslo, Norway). Cell pellet was resuspended in 1 ml RPMI at 1-2 × 10^6 cell/ml, and cell suspension was treated with 2 μl of a cell activation cocktail of phorbol-12myristate 13-acetate (40.5 μM) and ionomycin (669.3 μM) in DMSO (500x) and brefeldin A (BioLegend Inc., San Diego, CA, USA) for 6 hours at 37°C in a CO$_2$ incubator.

PBMCs were incubated with 5 μl of Human TruStain FcX™ (BioLegend Inc.) per million cells in 100 ml PBS for 10 minutes, and then, they were labeled with 5 μl of antihuman CD3-FITC-labeled, antihuman CD4-PeCy5-labeled, and antihuman CD161-APC-conjugated monoclonal antibodies (BD Biosciences, San Jose, CA); antihuman CD3-FITC-labeled, antihuman CD4-PeCy5-labeled, and antihu-

man CD25-APC-conjugated monoclonal antibodies (BD Biosciences); antihuman CD19-APC-labeled, antihuman CD24-FITC-conjugated, and antihuman CD38-PeCy5-labeled monoclonal antibodies (BD Biosciences); or antihuman CCR6-PerCP/Cy5.5-conjugated and antihuman CD123-FITC-labeled monoclonal antibodies (BD Biosciences) in separated tubes during 20 min at 37°C in the dark. Cells were permeabilized with 200 μl of cytofix/cytoperm solution (BD Biosciences) at 4°C for 30 min. Intracellular staining was performed with an anti-human IL-22-PE-, IL-17A-PE-, IL-4-PE-, IFN-γ-PE-, Foxp3-PE-, IL-10-PE-, and IDO-PE-labeled mouse monoclonal antibodies (BD Biosciences) for 30 min at 4°C in the dark. An electronic gate was made for CD3$^+$/CD4$^+$/CD161$^-$ cells, CD3$^+$/CD4$^+$/CD161$^+$ cells, CD3$^+$/CD4$^+$/CD25$^-$ cells, CD3$^+$/CD4$^+$/CD25^{hi} cells, CD19$^+$/CD38^{hi}/CD24^{hi} cells, and CD123^{hi}/CD196$^+$ cells. Results are expressed as the relative percentage of IL-22$^+$, IL-17A$^+$, IL-4$^+$, IFN-γ^+, Foxp3$^+$, IL-10$^+$, and IDO$^+$ expressing cells in each gate. As isotype control, IgG1-FITC/IgG1-PE/CD45-PeCy5 mouse IgG1 *kappa* (BD Tritest, BD Biosciences) was used to set the threshold and gates in the cytometer. We ran an unstained (autofluorescence control) and permeabilized PBMC sample. Autofluorescence control was compared to single-stained cell-positive controls to confirm that the stained cells were on scale for each parameter. Besides, BD Calibrate 3 beads were used to adjust instrument settings, set fluorescence compensation, and check instrument sensitivity (BD calibrates, BD Biosciences). Fluorescence minus one (FMO) controls were stained in parallel using the panel of antibodies with sequential omission of one antibody, except for the anti-IL-22, anti-IL-17A, anti-IL-4, anti-IFN-γ, anti-Foxp3, anti-IL-10, and anti-IDO antibody, which was replaced by an isotype control rather than simply omitted. Finally, T subsets were analyzed by flow cytometry with an Accuri C6 (BD Biosciences). A total of 500,000–1,000,000 events were recorded for each sample and analyzed with the FlowJo X software (Tree Star, Inc.) [26].

2.7. RNA Isolation and Quantitative Real-Time PCR Analyses of MicroRNAs.

Total serum RNA was isolated with TRIzol reagent (Invitrogen) according to the manufacturer's instructions. The concentration and quality of total RNA were measured by a NanoDrop 1000 Spectrophotometer (NanoDrop Technologies, Waltham, Mass). To quantify miRNAs, cDNA was synthesized using a Mir-X miRNA first-strand synthesis kit (Clontech) according to the manufacturer's instructions. Complementary DNA (cDNA) was amplified by real-time PCR with a SYBR green-based fluorescent method using the Maxima SYBR Green/ROX qPCR Master Mix (2X) (Thermo Scientific). U6 was used as an endogenous control to normalize the expression values. We chose the following panel of miRNAs, for their effect reported in the literature in the different regulatory cells studied here. Primer sequences used for real-time PCR were as follows: hsa-miR-21-5p, 5$'$-TAGCTTATCAGACTGATGTTGA-3$'$; hsa-miR-29a, 5$'$-TAGCACCATCTGAAATCGGTTA-3$'$; hsa-miR-29b, 5$'$-TAGC

ACCATTTGAAATCAGTGTT-3$'$; hsa-miR23b, 5$'$-TGGG TTCCTGGCATGCTGATTT-3$'$; hsa-miR-31, 5$'$-AGGC AAGATGCTGGCATAGCT-3$'$; hsa-miR-146a, 5$'$-TGAG AACTGAATTCCATGGGTT-3$'$; hsa-miR-155, 5$'$-TTAA TGCTAATCGTGATAGGGGT-3$'$; hsa-miR-150, 5$'$-TCTC CCAACCCTTGTACCAGTG-3$'$; hsa-miR-1246, 5$'$-AATG GATTTTTGGAGCAGG-3$'$; hsa-miR-197-3p, 5$'$TTCACC ACCTTCTCCACCCAGC-3$'$; hsa-miR-485-p, 5$'$AGAGGC TGGCCGTGATGAATTC-3$'$; and U6 forward, 5$'$-GCTT CGGCAGCACATATACTAAAAT-3$'$ and U6 reverse, 5$'$ -CGCTTCACGAATTTGCGTGTCAT-3$'$.

qRT-PCR assays were performed in a StepOne real-time PCR instrument (Life Technologies, Foster City, CA). The reactions were carried out with a 10 min incubation at 95°C followed by 40 cycles of 95°C for 15 s and 60°C for 1 min. All reactions were run in triplicate, and the average threshold cycle and SD values were calculated. The transcript levels were calculated based on the threshold cycle (C_t) using the delta-delta C_t method that measures the relative of a target RNA between two samples by comparing them to a normalization control RNA ($U6$).

2.8. Target Gene and Pathway Enrichment Analysis. We determined the gene targets of identified miRNAs using DIANA-TarBase v8 (http://www.microrna.gr/tarbase), which is a database containing experimentally validated miRNA-target interactions. We used DIANA-miRPath v3.0 (http://www.microrna.gr/miRPathv3) and the Kyoto Encyclopedia of Genes and Genomes (KEGG) database for the identification of the networks and pathway enrichment of the selected miRNA target genes. Enriched pathways showing statistical significance ($P \leq 0.05$) were subjected to further molecular analysis and interactome network construction. Interactome networks were constructed to connect miRNAs to their putative target genes (or to enrichment pathways) within the selected enriched pathways; the resulting networks were exported to Cytoscape v3.1.0 (http://cytoscape.org/index.php) for visualization.

2.9. Ethical Considerations. This work was performed according to the principles expressed in the Declaration of Helsinki. The study was approved (Reference 822) by the Ethical Committee from the Instituto Nacional de Ciencias Médicas y Nutrición Salvador Zubirán, and a written informed consent was obtained from all subjects.

2.10. Statistical Analysis. Descriptive statistic was performed, and categorical variables were compared using the Chi-2 test or Fisher's exact test. We used Mann-Whitney U-test for comparison of two medians. One-way analysis of variance on ranks Kruskal-Wallis, if the Kruskal-Wallis test was significant, a post hoc analysis (Dunn's test) was performed for all pairwise multiple comparison procedures. The relative expression of miRNAs was reported as medians and ranges (5th/95th percentiles). We reported nonparametric correlations using Spearman coefficients among serological relative expression of miRNAs and CLASI score. A strong correlation was defined as a Spearman coefficient between ±0.50 and ±1,

a medium correlation between ±0.30 and ±0.49, and a weak correlation below 0.29. We also performed a multiple linear regression analysis to evaluate the possible association of the meaningful miRNAs and the peripheral and skin cell subpopulations among CLE varieties.

All the statistical tests were performed 2-sided; P values less than 0.05 were considered statistically significant. SPSS (v. 21.0) and GraphPad Prism (v. 5) software was used for statistical analysis.

3. Results

3.1. Clinical and Demographic Characteristics. Clinical and demographic characteristics of the groups are summarized in Table 1. Most of the participants were females and had a similar age. We did not find significant differences regarding SLE duration, prednisone dose, and use of antimalarials and immunosuppressants among the groups with CLE. However, as expected, the median of the CLASI activity score in SCLE patients was higher than the score of DLE patients.

3.2. miRNA Profiling in SCLE and DLE Patients. The analysis revealed differential circulating levels of six miRNAs (miR-150, miR-23b, miR-1246, miR-21, miR-31, and miR-146) among the patients' groups and controls (Figure 1). In this regard, circulating levels of miR-1246 (372.7-fold decrease), miR-150 (183.1-fold decrease), miR-21 (14.7-fold decrease), miR-23b (14-fold decrease), and miR-146 (13-fold decrease) were considerably lower in patients with SCLE than in healthy controls. Patients with DLE also had lower levels of miR-21 (4.6-fold decrease), miR-1246 (3.8-fold decrease), and miR-150 (1.7-fold decrease) than healthy controls. When we compared the group with SCLE versus DLE, the SCLE group had lower levels of miR-1246 (75.5-fold decrease), miR-146 (40.6-fold decrease), and miR23b (23.2-fold decrease).

3.3. Correlation between miRNAs and CLASI Activity Score. Except for miR-150 in the subgroup of patients with SCLE ($\rho = -0.64$ CI 95% -0.78 to -0.11, $P = 0.01$), we did not find any correlation among the CLASI activity score and other circulating miRNA levels.

3.4. Associations of miRNAs and Circulating and Skin Cell Subpopulations. We performed a multiple regression analysis to evaluate the association of the different miRNAs and the circulating and skin cell subsets.

At peripheral blood, in the group of SCLE, we observed a negative association with CD4$^+$/CD25$^-$/IL-4$^+$ cells and CD4$^+$/CD25^{hi}/Foxp3$^+$ and miR-23b (Figures 2(a), 2(e), and 2(g), Table 2) and CD4$^+$/CD25$^-$/IFN-γ^+ with miR-1246 (Figures 2(a) and 2(f), Table 2). In the group of DLE patients, there was a positive association with CD123$^+$/CD196$^+$/IDO$^+$ plasmacytoid dendritic cells with miR-150 (Figures 2(b) and 2(i), Table 3).

At the skin, in the group of SCLE, a positive association was determined between miR-21 and CD4$^+$/IL-4$^+$ (Figure 3(c), Table 2); and CD20$^+$/IL-10$^+$ (Figure 3(f), Table 2) and CD4$^+$/IFN-γ^+ with miR-31 (Figure 3(d), Table 2). In the DLE patients' group, CD4$^+$/IL-4$^+$ cells were

TABLE 1: Clinical characteristics from patients with cutaneous lupus erythematosus.

	Cutaneous lupus erythematosus		Healthy donor $n = 19$	P value
	SCLE $n = 22$	DLE $n = 20$		
Demographics				
Age (years)				
Mean ± SD	38.2 ± 13.6	37.4 ± 15.3	43.6 ± 16.5	
Median	34.5	32.5	45.0	
Range	(20-62)	(18-74)	(21-76)	
Sex, females, (%)	95.5	95	95	
Disease duration (years)				
Mean ± SD	10.2 ± 10.3	7.5 ± 6.4	–	
Median	6.0	7.0		
Range	(1-41)	(1-26)		
Laboratory variables				
Hemoglobin (g/dl)				
Mean ± SD	12.6 ± 2.0	13.4 ± 1.5	14.4 ± 1.0	
Median	13.0	13.2	14.5	
Range	(9.3-15.8)	(11.2-16.5)	(12.5-15.8)	
Leucocytes (cells/μl)				
Mean ± SD	4905 ± 1951	4944 ± 1311	5649 ± 2102	
Median	4900	4900	5500	
Range	(1700-9100)	(2400-7000)	(1140-8200)	
Lymphocytes (%)				
Mean ± SD	19.1 ± 7.44	21.9 ± 5.2	30.4 ± 10.6	
Median	19.0	22.7	29.9	
Range	(8.0-33.0)	(14.9-33.5)	(18.1-47.2)	
Monocytes (%)				
Mean ± SD	9.3 ± 3.7	7.7 ± 2.6	6.8 ± 2.7	
Median	9.1	8.2	6.7	
Range	(4.4 – 15.0)	(3.0 – 13.1)	(1.0 – 10.3)	
Neutrophils (%)				
Mean ± SD	70.6 ± 8.3	68.1 ± 6.5	59.4 ± 10.7	
Median	72.6	67.6	62.5	
Range	(53.0–82.7)	(53.6–8.8)	(43.5–73.3)	**0.003**

TABLE 1: Continued.

|	Cutaneous lupus erythematosus		Healthy donor n = 19	P value
	SCLE n = 22	DLE n = 20		
Platelets (x10³cells/μl)				
Mean ± SD	191.6 ± 83.1	204.9 ± 49.4	241.8 ± 34.9	
Median	205.0	223.5	249.0	
Range	(30–360)	(128–276)	(192–306)	
C3 (mg/dl)			–	
Mean ± SD	73.2 ± 31.8	82.3 ± 28.1		
Median	68.5	78.7		
Range	(29.4-130.4)	(28.8-132.4)		
C4 (mg/dl)			–	
Mean ± SD	16.4 ± 9.9	15.2 ± 5.9		
Median	13.5	14.3		
Range	(5.9-37.2)	(6.0-29.0)		
Anti-dsDNA (IU/ml)			–	
Mean ± SD	135.6 ± 188.3	234.4 ± 363.5		
Median	49.0	12.5		
Range	(12.3-570.0)	(7.7-1116.7)		
Clinical variables				
CLASI activity score			–	0.01
Mean ± SD	20.9 ± 8.2	13.4 ± 6.3		
Median	20.0	12.5		
Range	(9–37)	(2-29)		
Treatment				
Antimalarial (%)	14 (63.6)	13 (65)	–	
Prednisone (mg/day)	10	15	–	
Immunosuppressants (%)	13 (59)	12 (60)	–	
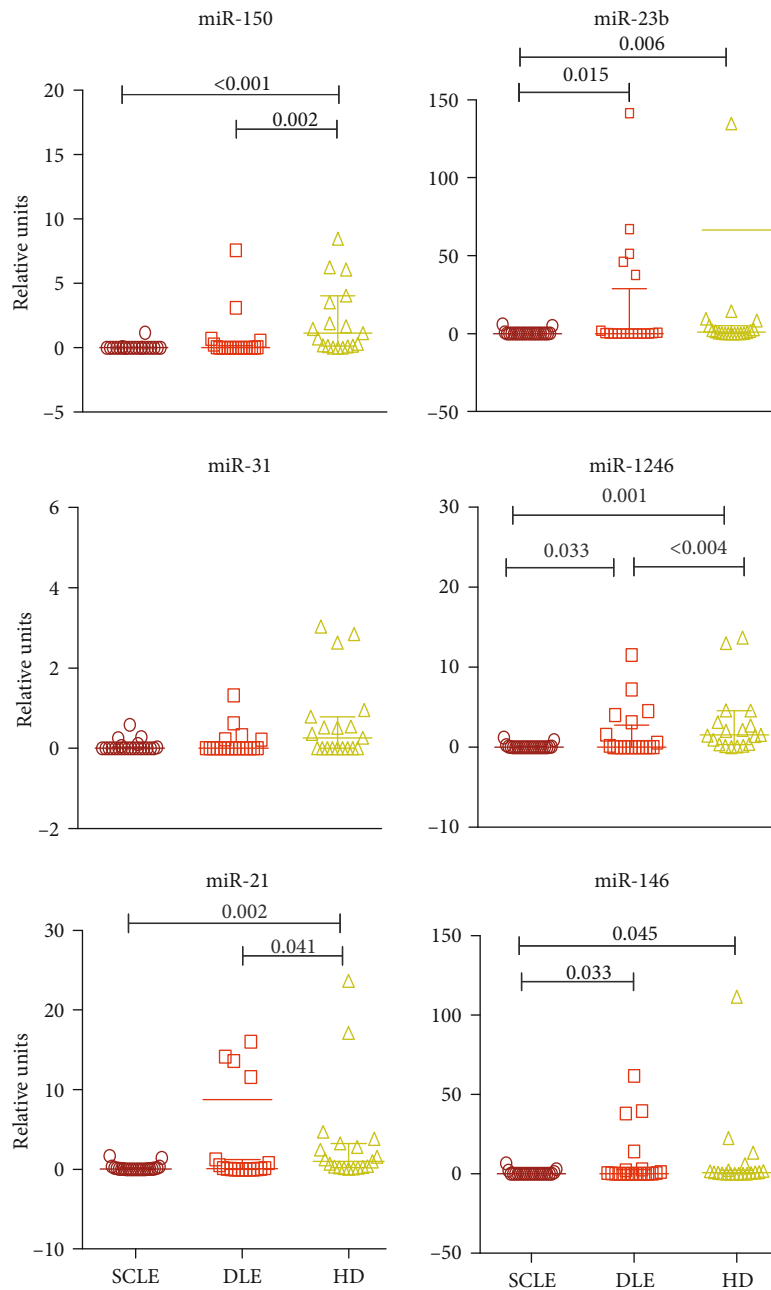
FIGURE 1: Expression of differentially expressed miRNAs in cutaneous lupus. *The results are expressed as the median and range (5th/95th percentiles). Kruskal-Wallis test and post hoc analysis (Dunn's test). SCLE: subacute cutaneous lupus erythematosus; DLE: discoid lupus erythematosus; HD: healthy donors.

associated positively with miR-150 (Figure 3(c), Table 3), and CD20$^+$/IL-10$^+$ cells with miR-1246 and miR-146a (Figure 3(f), Table 3).

3.5. Kyoto Encyclopedia of Genes and Genomes (KEGG) Pathway Enrichment Analysis of miRNAs Differentially Expressed in Patients with SCLE and DLE. The predicted targets and pathways of the differentially expressed miRNAs and their correlation with specific circulating and skin T cell subpopulations in both clinical conditions (SCLE: miR-21, miR-31, and miR-23b and DLE: miR-150, miR-1246, and miR-146a) were analyzed by using the KEGG pathway

enrichment strategy. The analysis of the predicted targets and pathways revealed that in SCLE, miR-21 was linked with Hippo signaling, bacterial invasion of epithelial cells, transcriptional regulation of cancer, prolactin signaling, FoxO signaling, and biosynthesis and degradation of fatty acids. Interestingly, miR-31 also was connected with cancer pathways associated with miR-21 and miR-23b. In addition, we found that miR-31 was significantly associated with TNF signaling.

Regarding DLE, miR-146a expression was significantly linked to immune relevant pathways including NF-kappa B signaling, Toll-like receptor signaling. miR-1246 was
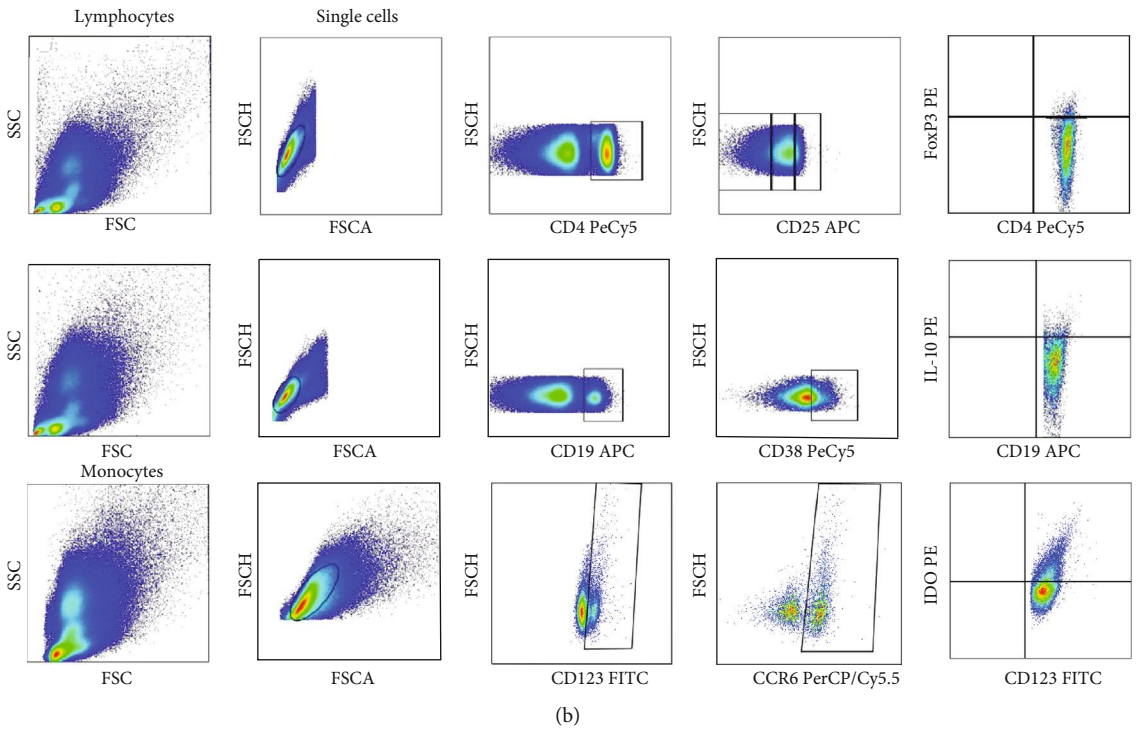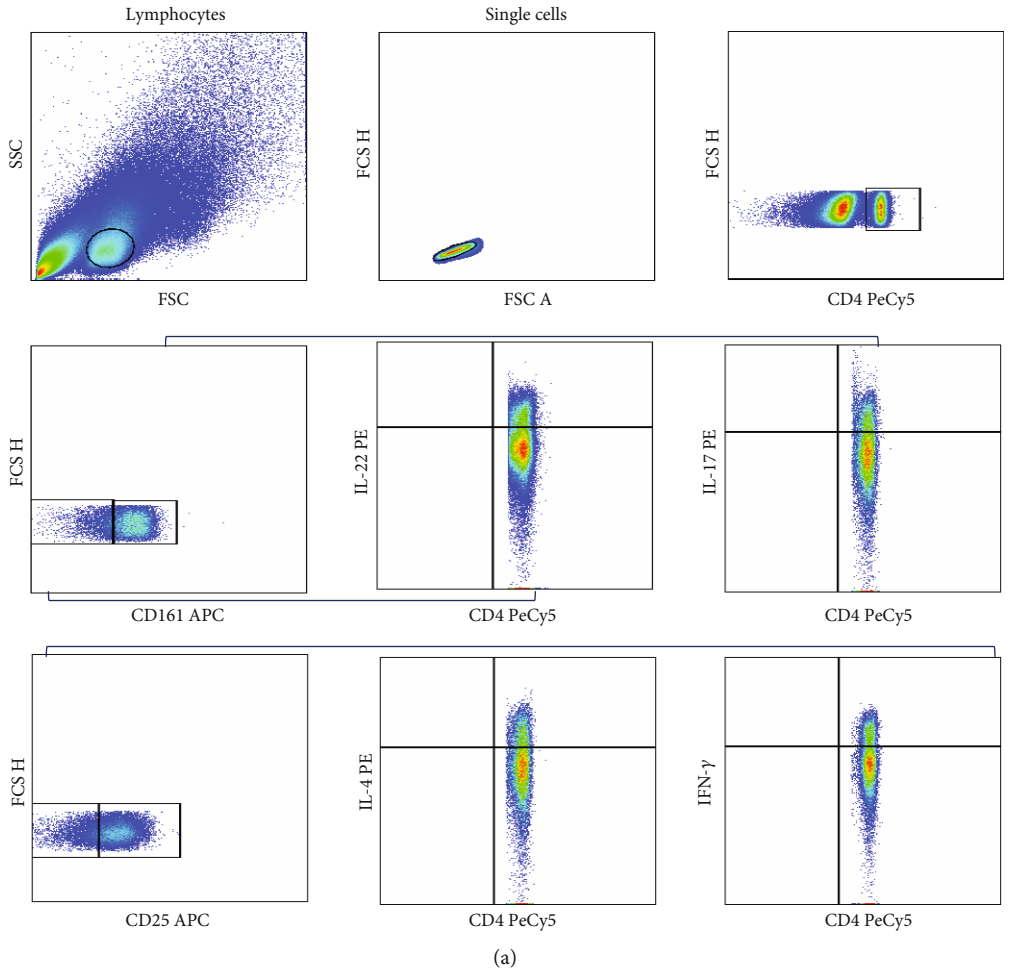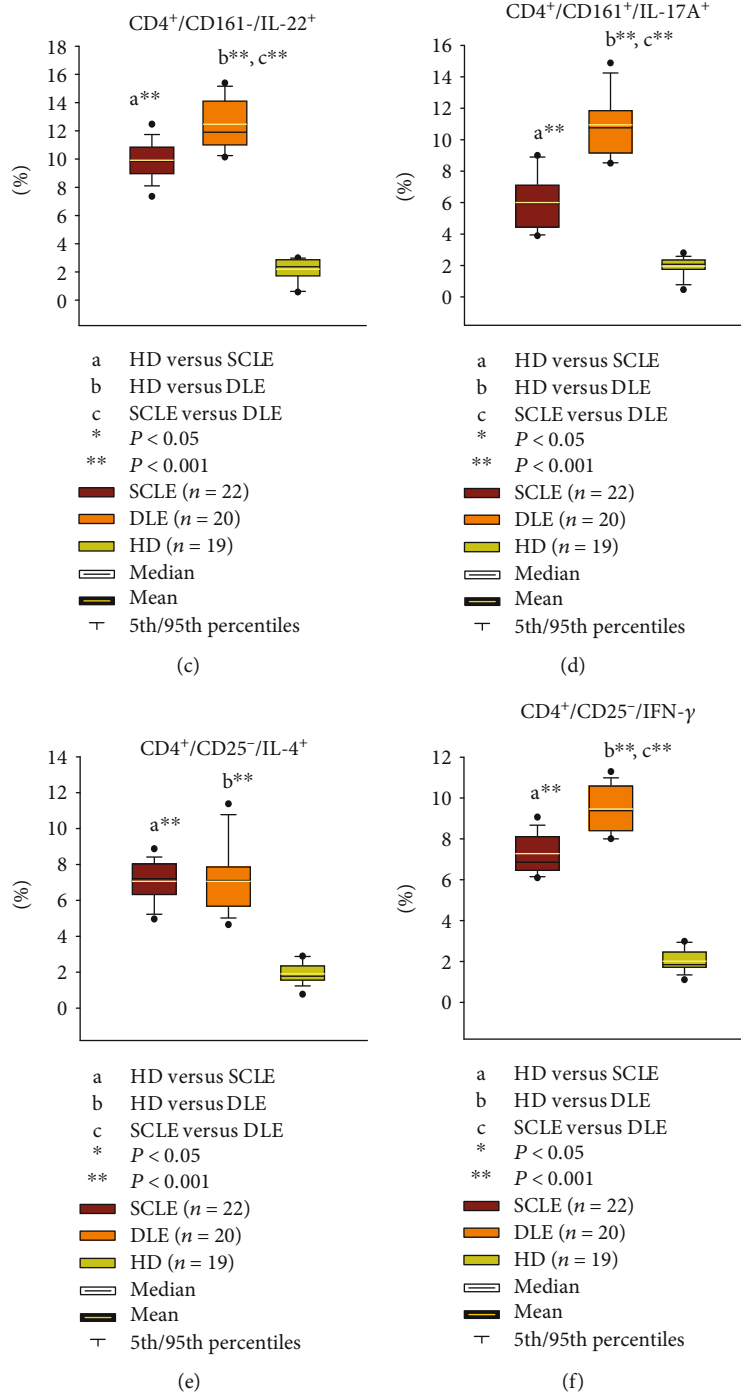
(a)

(b)

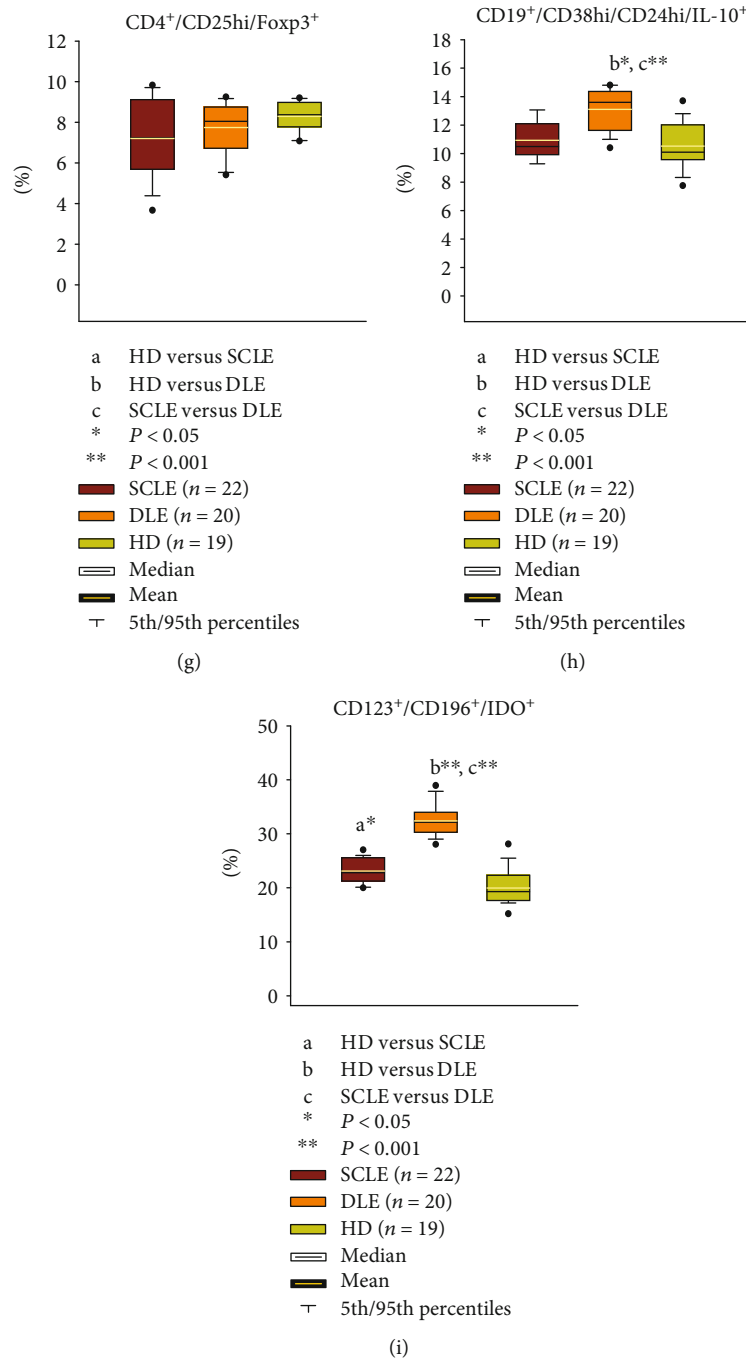Figure 2: Continued.

FIGURE 2: Continued.

(g)

(h)

(i)

FIGURE 2: (a) Representative gating strategy of each cell population of CD4 effector T cells. (b) Representative gating strategy of each cell population of regulatory cells of a DLE patient. Percentages of circulating (c) CD4$^+$/CD161$^-$/IL-22$^+$ cells, (d) CD4$^+$/CD161$^+$/IL-17A$^+$ cells, (e) CD4$^+$/CD25$^-$/IL-4$^+$ cells, (f) CD4$^+$/CD25$^-$/IFN-γ^+ cells, (g) CD4$^+$/CD25hi/Foxp3$^+$ cells, (h) CD19$^+$/CD38hi/IL-10$^+$ cells, and (i) CD123$^+$/CD196$^+$/IDO$^+$ cells. The results are expressed as the mean (horizontal yellow line), median (horizontal black line), and 5th/95th percentiles $^*P < 0.05$ and $^{**}P < 0.001$. SCLE: subacute cutaneous lupus erythematosus; DLE: discoid lupus erythematosus; HD: healthy donors.

associated with apoptosis and viral carcinogenesis. Finally, miR-150 in CLE was closely related to HIF-1 signaling and cancer pathways.

Interestingly, the interactome analysis showed a group of pathways that were linked with specific miRNAs expressed in SCLE and DLE patients. In this context, cell cycle regulation, p53 signaling, TGF-β signaling, thyroid hormone signaling, and cancer pathways were shared between miR-21, miR-31, and miR-23b (expressed in SCLE) and miR-146a, miR-1246, and miR-150 expressed in DLE patients (Figure 4).

TABLE 2: Multiple linear regression models for patients with SCLE.

	Model	miRNAs	R	R square	β	t	Sig. (P)	95% IC for β Lower	Up
Peripheral cells									
CD3$^{+/}$CD4$^+$/CD25$^-$/IL-4$^+$	1	miR-23b	0.493	0.244	-0.493	-2.407	0.027	-0.901	-0.061
CD3$^+$/CD4$^+$/CD25$^+$/IFN-γ$^+$	1	miR-1246	0.431	0.186	-0.431	-2.908	0.006	-0.399	-0.071
CD3$^+$/CD4$^+$/CD25hi/Foxp3$^+$	1	miR-23b	0.449	0.201	-0.449	-2.13	0.047	-1.47	-0.01
Tissue cells									
IL-4-expressing CD4$^+$ cells (epidermis)	1	miR-21	0.487	0.237	0.487	2.365	0.029	0.425	7.171
IFN-γ-expressing CD4$^+$ cells (dermis)	1	miR-31	0.467	0.218	0.467	2.238	0.038	0.717	22.62
IL-10-expressing CD20$^+$ cells (epidermis)	1	miR-21	0.492	0.242	0.492	2.396	0.028	0.61	9.298

SCLE: subacute cutaneous lupus erythematosus; DLE: discoid lupus erythematosus; HD: healthy donors.

TABLE 3: Multiple linear regression models for patients with DLE.

	Model	miRNAs	R	R square	β	t	Sig. (P)	95% IC for β Lower	Up
Peripheral cells									
CD123hi/CD196$^+$/IDO$^+$	1	miR-150	0.448	0.201	0.448	2.125	0.048	0.009	1.54
Tissue cells									
IL-4-expressing CD4$^+$ cells (dermis)	1	miR-150	0.517	0.267	0.517	2.562	0.020	0.27	2.728
	1	miR-1246	0.75	0.563	0.75	4.811	<0.001	0.613	1.563
IL-10-expressing CD20$^+$ cells (epidermis)	2	miR-1246	0.809	0.655	0.859	5.672	<0.001	0.782	1.709
		miR-146a			-0.322	-2.13	0.048	-0.165	-0.001
IL-10-expressing CD20$^+$ cells (epidermis)	1	miR-1246	0.736	0.542	0.736	4.611	<0.001	0.83	2.22
	2	miR-1246	0.673	0.634	0.866	5.874	<0.001	1.15	2.439
		miR-146a			-0.385	-2.612	0.018	-0.256	-0.027

SCLE: subacute cutaneous lupus erythematosus; DLE: discoid lupus erythematosus; HD: healthy donors.

Importantly, the degree of association between the differentially expressed miRNA signatures and specific T cell subpopulations observed in SCLE and DLE patients and their enrichment with the aforementioned pathways are shown in Figure 5. Detailed P values and the degree of association of specific miRNAs and functional pathways are enlisted in Figures S2 and S3.
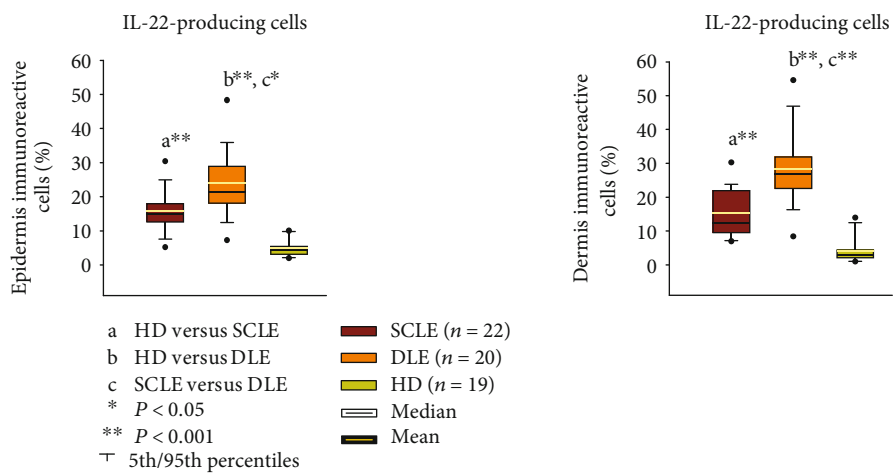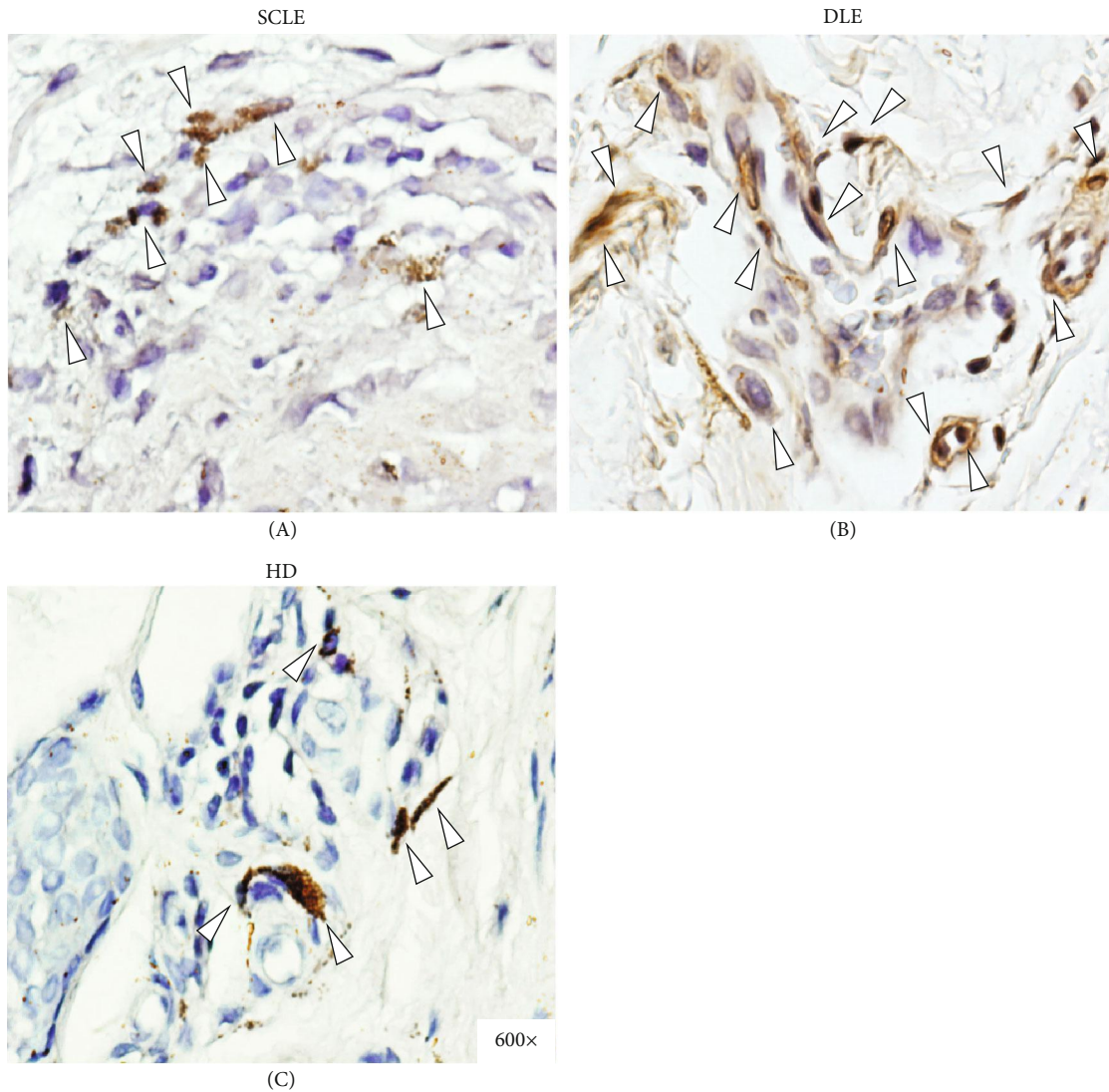
4. Discussion

miRNAs are key determinants in the posttranscriptional regulation of genome [27, 28] and are involved in the control of many biological processes including inflammation [29]. It is well known that an uncontrolled immune inflammatory response might contribute to the pathogenesis of autoimmunity.

In the present work, we explored if the expression of circulating miRNA signature might identify patients with CLE and their varieties, as was described by Solé et al. for miR-31 and miR-485-3p overexpression in DLE compared to SCLE [12]. Our most relevant findings were that miR-150, miR-1246, miR-21, miR-23b, and miR-146 were downregulated in SCLE than in healthy controls. Furthermore, miR-1246, miR-23b, and miR-146 expression was lower in SCLE than in DLE. We observed some differences regardi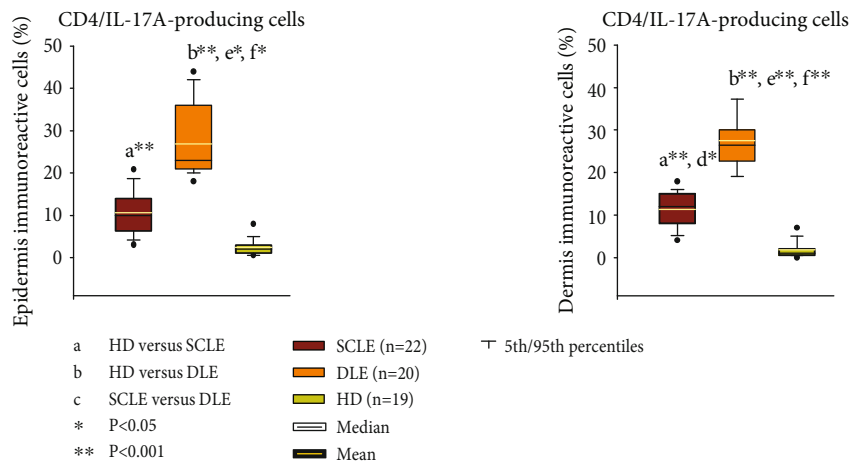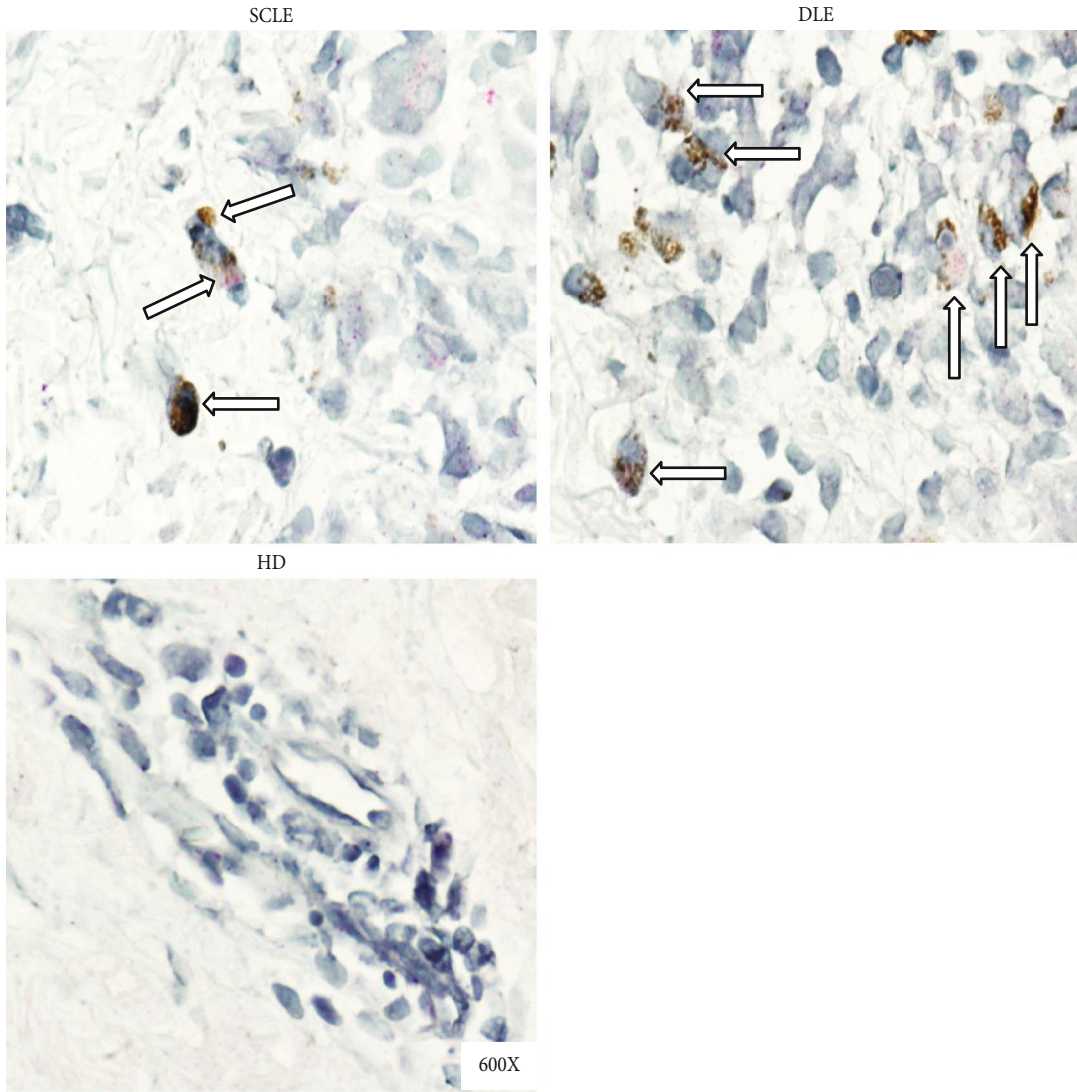ng the association of peripheral and tissue subpopulation expression and the miRNAs according to CLE varieties. Notwithstanding in the SCLE group, miR-23b and miR1246 drove a Th2 and Th1 peripheral response; whereas in the DLE group, miR-1246 was associated with infiltrates of IL-10-producing B cells.

miR-150 is expressed in different lineages of immune cells and is involved in cellular maturation from pro-B to pre-B lymphocytes, as well as in the development and functional activity of NK and iNKT cell lineages [30, 31]. Regarding the participation of miR-150 at the skin biology, it has been demonstrated that its downregulation promotes keratinocyte proliferation in hypoxic conditions through targeting HIF-1α and VEGF-A [32]. Besides, miR-150 downregulation is associated with the constitutive type I collagen overexpression in scleroderma dermal fibroblasts via the induction of integrin $β_3$ [33]. miR-150 seems to play an important role in the induction of myofibroblast proliferation and its resistance to apoptosis [34]. Moreover, miR-150 is also downregulated in other autoimmune diseases with skin involvement, including psoriasis and diffuse cutaneous systemic sclerosis (SSc) skin lesions [32]. Specifically, in SSc, downregulation promotes TGF-β signaling and Smad3 phosphorylation, resulting in the transcriptional activation of type I collagen gene and tissue fibrosis [32]. In this vein, a study described that patients with DLE exhibited a distinctive overexpression signature of profibrotic markers including TGF-β and
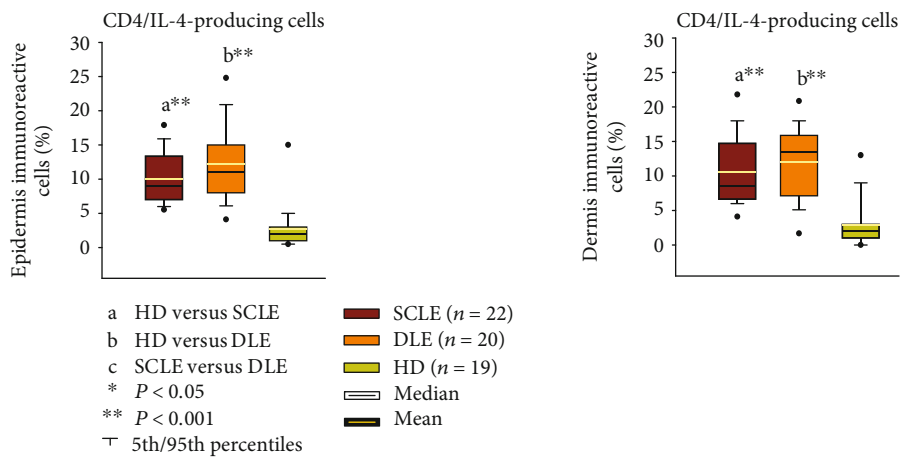
SCLE

(A)

DLE

(B)

HD

600×

(C)

IL-22-producing cells

IL-22-producing cells

a   HD versus SCLE
b   HD versus DLE
c   SCLE versus DLE
* $P < 0.05$
** $P < 0.001$
⊤   5th/95th percentiles

SCLE ($n = 22$)
DLE ($n = 20$)
HD ($n = 19$)
Median
Mean

(a)

FIGURE 3: Continued.

SCLE

DLE

HD

600X

CD4/IL-17A-producing cells

b**, e*, f*

a**

Epidermis immunoreactive cells (%)

CD4/IL-17A-producing cells

b**, e**, f**

a**, d*

Dermis immunoreactive cells (%)

a   HD versus SCLE
b   HD versus DLE
c   SCLE versus DLE
*   P<0.05
**   P<0.001

SCLE (n=22)
DLE (n=20)
HD (n=19)
Median
Mean

⊤ 5th/95th percentiles

(b)

FIGURE 3: Continued.

SCLE

(A)

DLE

(B)

HD

600×

(C)

CD4/IL-4-producing cells

CD4/IL-4-producing cells

a   HD versus SCLE
b   HD versus DLE
c   SCLE versus DLE
* $P < 0.05$
** $P < 0.001$
⊤ 5th/95th percentiles

SCLE ($n = 22$)
DLE ($n = 20$)
HD ($n = 19$)
Median
Mean

(c)

FIGURE 3: Continued.

(A)

(B)

(C)

600×

CD4/IFN-γ-producingcells

CD4/IFN-γ-producingcells

Epidermis immunoreactive cells (%)

Dermis immunoreactive cells (%)

a**

b**, c*

a**

b**, c*

a   HD versus SCLE

b   HD versus DLE

c   SCLE versus DLE

* $P < 0.05$

** $P < 0.001$

⊤   5th/95th percentiles

SCLE ($n = 22$)

DLE ($n = 20$)

HD ($n = 19$)

Median

Mean

(d)

FIGURE 3: Continued.

(A)

(B)

(C)

600×

(e)

FIGURE 3: Continued.

SCLE

(A)

DLE

(B)

HD

600×

(C)

CD20/IL-10-producing cells

CD20/IL-10-producing cells

a HD versus SCLE
b HD versus DLE
c SCLE versus DLE
* $P < 0.05$
** $P < 0.001$
⊤ 5th/95th percentiles

SCLE ($n = 22$)
DLE ($n = 20$)
HD ($n = 19$)
Median
Mean

(f)

Figure 3: Continued.

(A)

(B)

(C)

FIGURE 3: Continued.

(h)

IL-22-producing cells

(h′)

IL-22-producing cells

(h)

(i)

CD4/IL-17A-producing cells

(i′)

CD4/IL-17A-producing cells

(i)

(j)

CD4/IL-4-producing cells

(j′)

CD4/IL-4-producing cells

a   HD versus SCLE   SCLE ($n = 22$)
b   HD versus DLE   DLE ($n = 20$)
c   SCLE versus DLE   HD ($n = 19$)
* $P < 0.05$ Median
** $P < 0.001$ Mean
⊤   5th/95th percentiles

(j)

Figure 3: Continued.

(k)

CD4/IFN-γ-producingcells

(k')

CD4/IFN-γ-producingcells

a HD versus SCLE
b HD versus DLE
c SCLE versus DLE
* $P < 0.05$
** $P < 0.001$
⊤ 5th/95th percentiles

☐ SCLE ($n = 22$)
☐ DLE ($n = 20$)
☐ HD ($n = 19$)
☐ Median
☐ Mean

(k)

(l)

CD25/Foxp3-producing cells

(l')

CD25/Foxp3-producing cells

a HD versus SCLE
b HD versus DLE
c SCLE versus DLE
* $P < 0.05$
** $P < 0.001$
⊤ 5th/95th percentiles

☐ SCLE ($n = 22$)
☐ DLE ($n = 20$)
☐ HD ($n = 19$)
☐ Median
☐ Mean

(l)

(m)

CD20/IL-10-producing cells

(m')

CD20/IL-10-producing cells

a HD versus SCLE
b HD versus DLE
c SCLE versus DLE
* $P < 0.05$
** $P < 0.001$
⊤ 5th/95th percentiles

☐ SCLE ($n = 22$)
☐ DLE ($n = 20$)
☐ HD ($n = 19$)
☐ Median
☐ Mean

(m)

Figure 3: Continued.

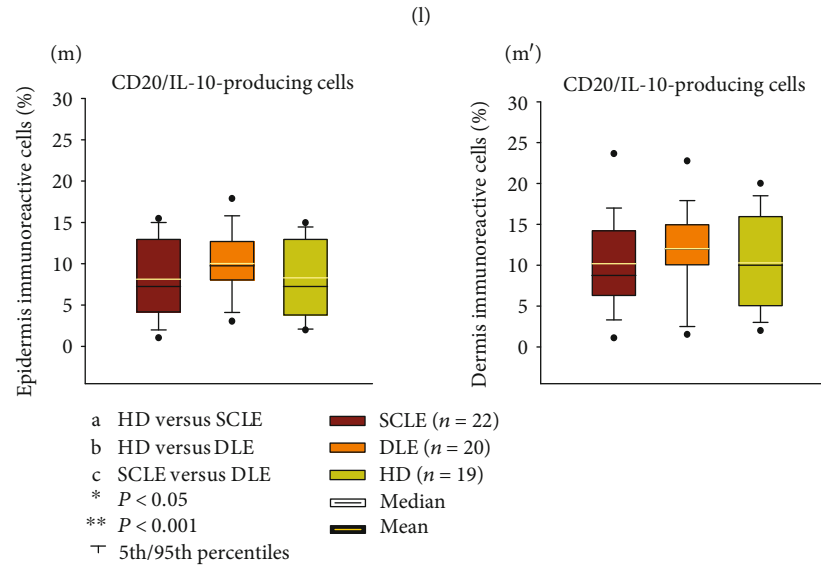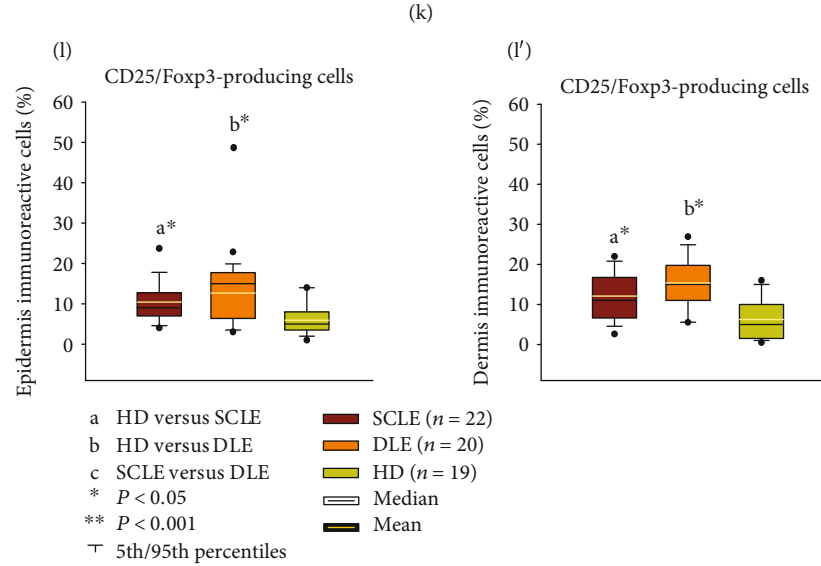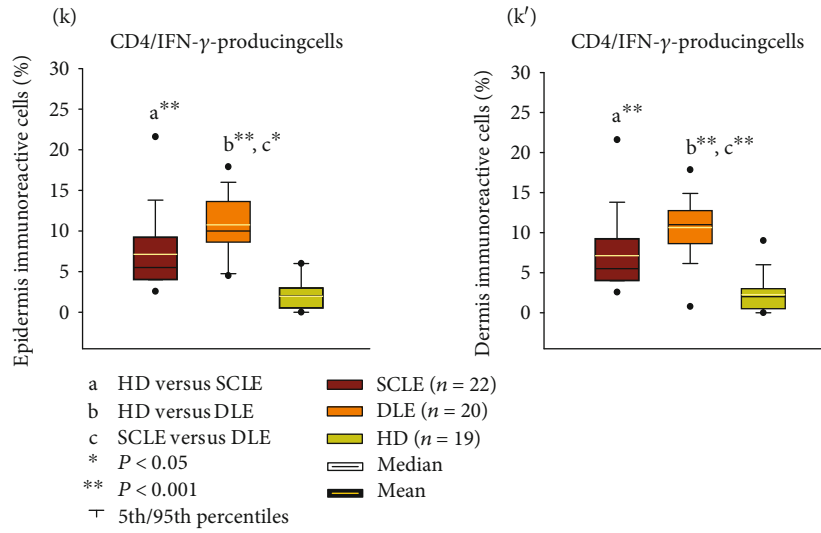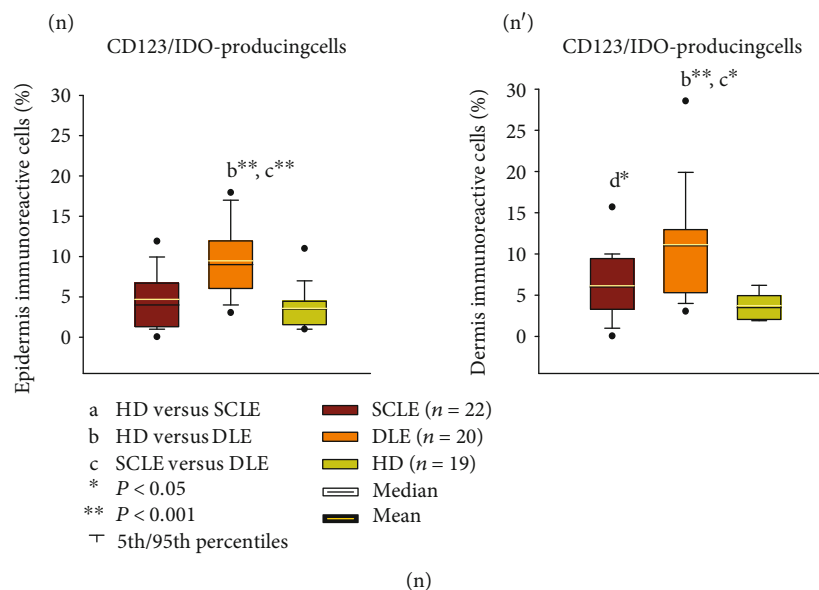FIGURE 3: Representative immunostaining of (a) IL-22-expressing cells, (b) IL-17A-expressing CD4 T cells, (c) IL-4-expressing CD4 T cells, (d) IFN-γ-expressing CD4 T cells, (e) Foxp3-expressing CD25 T cells, (f) IL-10-expressing CD20 B cells, and (g) IDO-expressing CD123 plasmacytoid dendritic cells in tissue biopsies from subacute cutaneous lupus erythematosus ((A) SCLE), discoid lupus erythematosus ((B) DLE), healthy donors ((C) HD). Arrowheads show single staining (in brown or red), and arrows depict double staining (in burgundy). Original magnification was ×600. (h–n) Percentage of immunoreactive cells per microscopic field. The results are expressed as the mean (horizontal yellow line), median (horizontal black line), and 5th/95th percentiles. $^*P < 0.05$ and $^{**}P < 0.001$. SCLE: subacute cutaneous lupus erythematosus; DLE: discoid lupus erythematosus; HD: healthy donors.

SMAD3 [12]. Also, in line with these studies, our findings suggest that the downregulation of miR-150 in CLE might influence the activation of chronic inflammatory and profibrotic pathways.

On the other hand, the role of miR-1246 in normal skin and autoimmune disorders is still poorly characterized. In patients with SLE, it was found downregulated. This low expression might be related to commitment hyperactivation of B cells. Interestingly, B cells from nonactive SLE patients have similar expression levels of miR-1246 when compared with healthy volunteers [17]. Moreover, it has been demonstrated that miR-1246 promotes UVB-induced apoptosis by downregulating RTKN2 expression in keratinocytes [35]. Herein, we observed that this miRNA was also downregulated in patients with SCLE and DLE.

Concerning miR-146, it has been observed that melanoma lesions overexpress it [36]. In patients with psoriasis, miR-146a is positively correlated with IL-17 expression in skin lesions and PBMCs [37]. Furthermore, miR-146a regulates the proinflammatory TLR/MyD88 pathway by targeting IRAK1 and TRAF6 [38]. miR-146a also contributes to the development of SLE, due to the reason that it is a negative regulator of type I IFN pathway by targeting IRF5, STAT1, IRAK1, and TRAF6 [34]. As in patients with SLE, herein, we observed a downexpression in CLE. Thus, the decreased expression of miR-146a in PBMCs might contribute to the enhanced production of type I IFN (IFN-α/β) in human lupus.

miR-23b, which is a differentiation marker of human keratinocytes (through repression of TGIF1 and activation

of the TGF-β-SMAD2 signaling pathway), is remarkably upregulated after UVA irradiation of human primary keratinocytes and acts through targeting-related RAS viral oncogene homolog 2 (RRAS2), which is strongly expressed in highly aggressive malignant skin cancer [39, 40]. Moreover, miR-23b promotes cutaneous wound healing through inhibition of the inflammatory responses by targeting ASK1 [41].

Furthermore, we reported a downexpression of miR-21 among CLE patients but not of miR-31. miR-21, as well as miR-31, are master regulators of T cell activation in SLE [42]. Several studies have demonstrated that aberrant expression of miR-21 is involved in the pathogenesis of SSc and psoriasis. miR-21 regulates genes such as SMAD3, SMAD7, and type I collagen, all involved in fibrosis [34]. Moreover, it has been demonstrated a reciprocal regulation between thyroid hormone and miR-21 where miR21 downregulates hedgehog pathway-driven skin tumorigenesis (basal cell carcinoma) [43]. Overexpression of miR-21 also inhibits the growth and metastasis of melanoma cells by targeting MKK3 [44].

In SLE patients, miR-31 was downregulated and negatively associated with disease activity and proteinuria, whereas miR-21 high expression correlated with the SLEDAI score and proteinuria. In addition, a reduced expression of miR-31 appears to alter the production of IL-2 by T cells in SLE patients, possibly influencing the expression of nuclear factor of activated T cells (NFAT) [45].

On the other hand, a recent study described a specific miRNA skin signature for DLE that included miR-31 and miR-485-3p. It demonstrated that the overexpression of
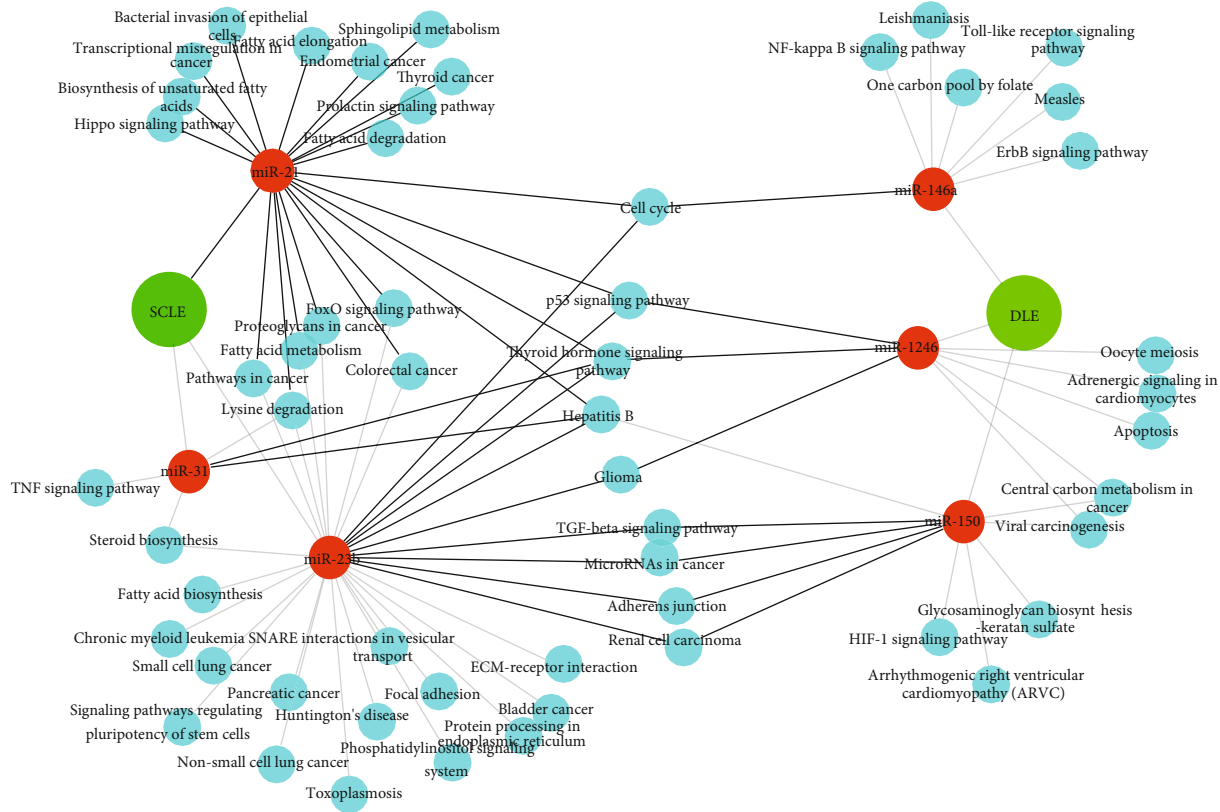
Figure 4: Interactome analysis of the most significantly enriched networks of differentially expressed miRNAs in SCLE and DLE patients. miR-21, miR-31, and miR-23b (red circles) are strongly associated with SCLE whereas miR-146a, miR-1246, and miR-150 (red circles) are linked with DLE. Significantly associated pathways enriched in KEGG analysis of these miRNA signatures are also shown in dark green circles.

miR-31 was stimulated by UV and TGF-β and this miRNA activated NF-κB signaling stimulating proinflammatory responses resulting in neutrophil and macrophage infiltrates in skin [2]. miR-31 is a key regulator for promoting keratinocyte proliferation and migration during wound healing [46], and it is overexpressed in SSc, a systemic disease characterized by extensive fibrosis [47, 48].

Finally, the participation of some immune response pathways including PRR signaling, JAK-signal transducer, STAT signaling, NF-κB signaling, and mitogen-activated protein kinase (MAPK) signaling cascade has been described in CLE [5]. Herein, several pathways were linked with the circulating miRNAs differentially expressed in CLE. Interactome network analysis revealed a strong connection between circulating miRNAs in SCLE and DLE groups with a particularly solid network connection such as cell cycle regulation pathways, p53 signaling, TGF-β signaling, NF-κB signaling, HIF-1 pathway, thyroid hormone signaling, and cancer pathways, among others. Some of them, as previously mentioned, had been described in CLE, but others did not, opening new areas of research. Overall, new insights into the pathogenesis of CLE might allow the development of new target treatments such as the inhibition of these immune pathways.

Certainly, we acknowledge that our study has the following limitations: first, a limited sample size and the lack of a replication cohort. Notwithstanding, our sample was carefully clinically selected and was able to detect differences in the expression of miRNAs among the different groups of CLE patients. Second, we did not evaluate the presence of miRNAs in skin biopsies. However, we were interested in studying circulating miRNAs with the purpose of further using them as future potential blood-based biomarkers to assess relapses and response to treatment, without the need of a skin biopsy. Finally, at the analysis of peripheral and skin subpopulations, none of the downregulated circulating miRNAs were associated with Th17 and Th22 cells previously recognized as participants in CLE pathogenesis. Thus, it is highly probable that other miRNAs might be also implicated in the regulation of these cell subpopulations. Besides these limitations, we consider that our current manuscript is of relevance particularly for the scant information regarding the pathogenesis of CLE.

Summing up, we determined downregulation of miR-150, miR-1246, and miR-21 in CLE patients. SCLE variety had the lowest levels of miR-1246, miR-146, and miR-23b. Overall, these miRNAs drove the presence of different peripheral and skin subpopulations and participated in diverse pathways. Further research is needed to validate our results in other populations and to evaluate the role of these miRNAs as clinical biomarkers.
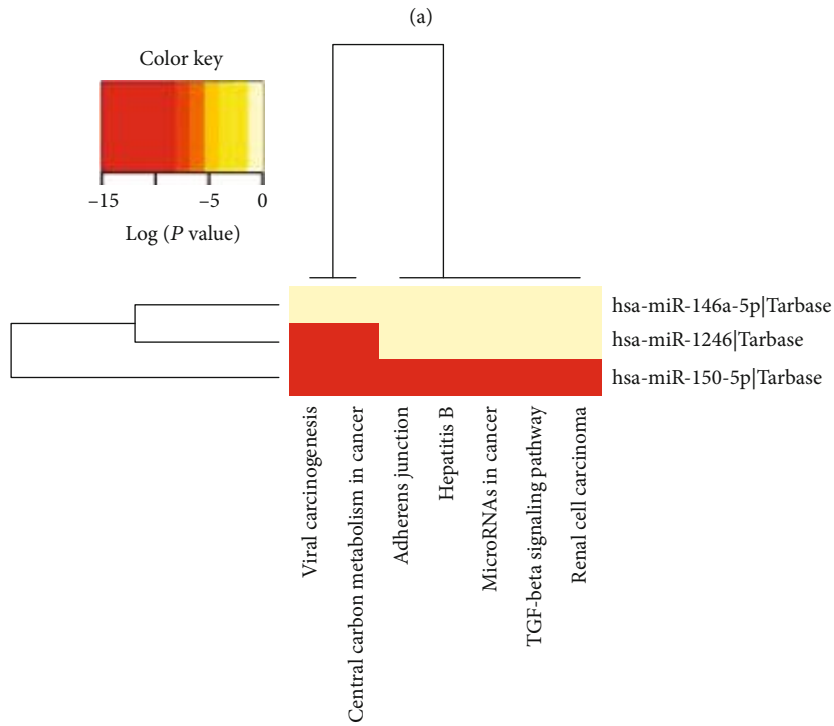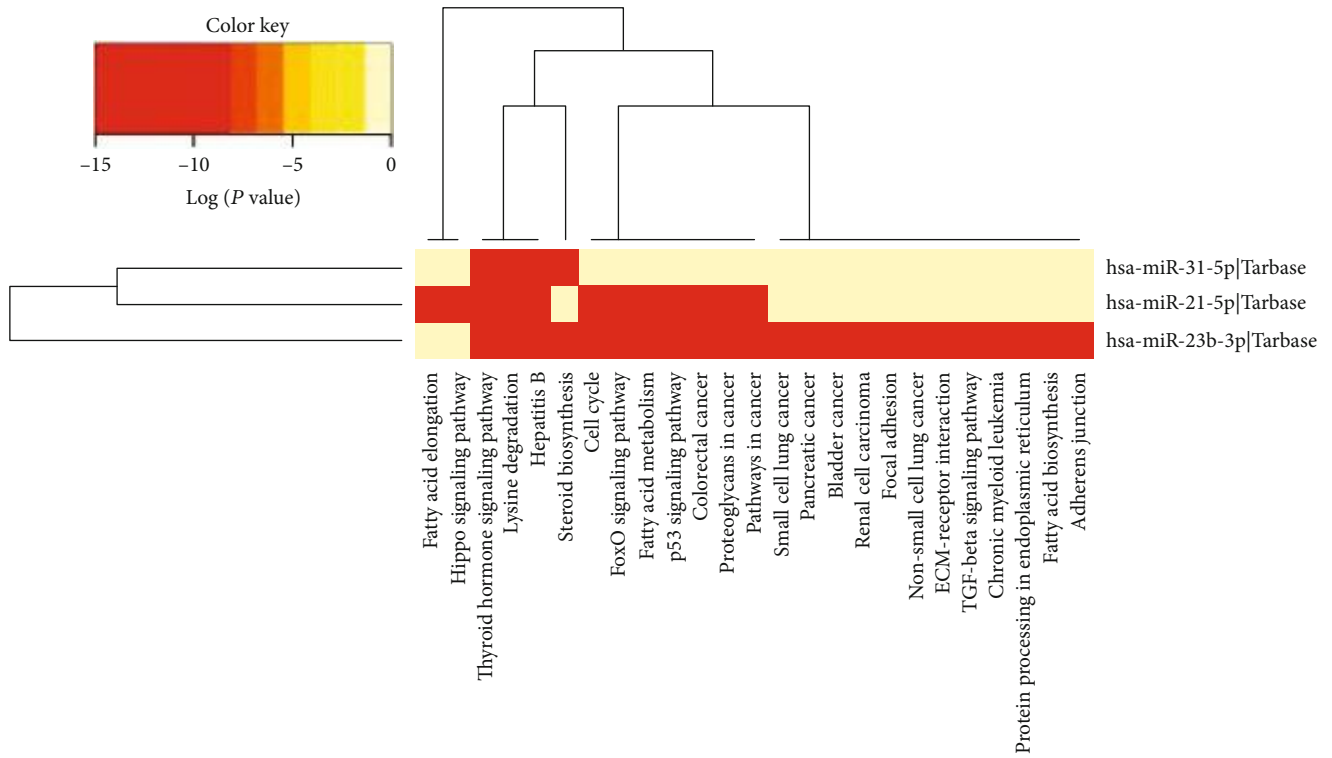
(a)

(b)

FIGURE 5: (a) Heat map of KEGG pathways enriched with gene regulated by a combination of hsa-miR-23b-3p, hsa-miR-21-5p, and hsa-miR-31-5p (SCLE); (b) heat map of KEGG pathways enriched with gene regulated by a combination of hsa-miR-150-5p, hsa-miR-1246, and hsa-miR-146a-5p (DLE).

Data Availability

Data will be provided based on requirement.

Additional Points

What Is Already Known About This Topic. (1) Cutaneous lupus erythematosus (CLE) is an autoimmune condition that comprehends a wide range of dermatological manifestations that can appear independently, or precede, systemic lupus erythematosus. (2) The pathogenesis of CLE is multifactorial and involves genetic predisposition, environmental factors, and abnormalities in the innate and adaptive immune response. (3) Recent studies have revealed the potential contribution of miRNAs in the regulation of signaling pathways. *What Does This Study Add.* (1) Circulating miR-150, miR-1246, and miR-21 were decreased in CLE patients. (2) SCLE variety was associated with lower levels of miR-21, miR-23b, and miR-31. (3) DLE variety was associated with lower levels of miR-146, miR-150, and miR-1246. These miRNAs drove the presence of different peripheral and skin subpopulations and participated in diverse pathways. *What Is the Translational Message.* (1) Circulating miRNAs could be used as future potential blood-based biomarkers to assess relapses and response to treatment, without the need of a skin biopsy. (2) Regulation of circulating miRNAs could be useful in the treatment of CLE.

Conflicts of Interest

The authors declare that they have no competing interests.

Authors' Contributions

SMF obtained patient consent to participate, followed up the patients, gathered clinical information tissue and blood samples, performed experiments, analyzed data, and wrote the manuscript. GRM, LJA, ACL, NERZ, and BOQ performed experiments, analyzed data, and wrote the manuscript. JZ, GHM, and JFC designed the study, performed experiments, supervised the research, analyzed the data, and wrote the manuscript.

Acknowledgments

Supplementary Materials

Supplementary Figure 1: representative immunostaining of (a) IL-22-expressing cells, (b) IL-17A-expressing cells, (c) IL-4-expressing cells, (d) IFN-γ-expressing cells, (e) Foxp3-expressing cells, (f) IL-10-expessing cells, and (g) IDO-expressing cells in tissue biopsies from spleen. Original magnification was ×600. Supplementary Figure 2: heat map of KEGG pathways enriched with gene regulated by a combination of hsa-miR-150-5p, hsa-miR-1246, and hsa-miR-146a-5p in patients with DLE. Supplementary Figure 3: heat map of KEGG pathways enriched with gene regulated by a combination of hsa-miR-23b-3p, hsa-miR-21-5p, and hsa-miR-31-5p in patients with SCLE. *(Supplementary Materials)*

References

[1] M. G. Kirchhof and J. P. Dutz, "The immunopathology of cutaneous lupus erythematosus," *Rheumatic Diseases Clinics of North America*, vol. 40, no. 3, pp. 455–474, 2014.

[2] A. Kuhn, D. Bein, and G. Bonsmann, "The 100th anniversary of lupus erythematosus tumidus," *Autoimmunity Reviews*, vol. 8, no. 6, pp. 441–448, 2009.

[3] Y. Zhang, J. Wu, Y. F. Han, Z. R. Shi, and L. Wang, "Pathogenesis of cutaneous lupus erythema associated with and without systemic lupus erythema," *Autoimmunity Reviews*, vol. 16, no. 7, pp. 735–742, 2017.

[4] S. Méndez-Flores, G. Hernández-Molina, A. B. Enríquez et al., "Cytokines and effector/regulatory cells characterization in the physiopathology of cutaneous lupus erythematous: a cross-sectional study," *Mediators of Inflammation*, vol. 2016, Article ID 7074829, 15 pages, 2016.

[5] J. Wenzel, "Cutaneous lupus erythematosus: new insights into pathogenesis and therapeutic strategies," *Nature Reviews Rheumatology*, vol. 15, no. 9, pp. 519–532, 2019.

[6] R. Dai and S. A. Ahmed, "MicroRNA, a new paradigm for understanding immunoregulation, inflammation, and autoimmune diseases," *Translational Research*, vol. 157, no. 4, pp. 163–179, 2011.

[7] D. T. Gracias and P. D. Katsikis, "MicroRNAs: key components of immune regulation," *Advances in Experimental Medicine and Biology*, vol. 780, pp. 15–26, 2011.

[8] B. Zhang, Q. Wang, and X. Pan, "MicroRNAs and their regulatory roles in animals and plants," *Journal of Cellular Physiology*, vol. 210, no. 2, pp. 279–289, 2007.

[9] S. O. Steen, L. V. Iversen, A. L. Carlsen et al., "The circulating cell-free microRNA profile in systemic sclerosis is distinct from both healthy controls and systemic lupus erythematosus," *The Journal of Rheumatology*, vol. 42, no. 2, pp. 214–221, 2015.

[10] G. Wang, L. S. Tam, E. K. Li et al., "Serum and urinary free microRNA level in patients with systemic lupus erythematosus," *Lupus*, vol. 20, no. 5, pp. 493–500, 2011.

[11] Y. Dai, Y. S. Huang, M. Tang et al., "Microarray analysis of microRNA expression in peripheral blood cells of systemic lupus erythematosus patients," *Lupus*, vol. 16, no. 12, pp. 939–946, 2007.

[12] C. Solé, S. Domingo, B. Ferrer, T. Moliné, J. Ordi-Ros, and J. Cortés-Hernández, "MicroRNA expression profiling identifies miR-31 and miR-485-3p as regulators in the pathogenesis of discoid cutaneous lupus," *The Journal of Investigative Dermatology*, vol. 139, no. 1, pp. 51–61, 2019.

[13] X. Wang, C. Zhang, Z. Wu, Y. Chen, and W. Shi, "CircIBTK inhibits DNA demethylation and activation of AKT signaling pathway via miR-29b in peripheral blood mononuclear cells in systemic lupus erythematosus," *Arthritis Research & Therapy*, vol. 20, no. 1, p. 118, 2018.

[14] A. Liston, A. S. Papadopoulou, D. Danso-Abeam, and J. Dooley, "MicroRNA-29 in the adaptive immune system:

setting the threshold," *Cellular and Molecular Life Sciences*, vol. 69, no. 21, pp. 3533–3541, 2012.

[15] L. P. Tan, M. Wang, J. L. Robertus et al., "miRNA profiling of B-cell subsets: specific miRNA profile for germinal center B cells with variation between centroblasts and centrocytes," *Laboratory Investigation*, vol. 89, no. 6, pp. 708–716, 2009.

[16] S. Zhu, W. Pan, X. Song et al., "The microRNA miR-23b suppresses IL-17-associated autoimmune inflammation by targeting TAB2, TAB3 and IKK-α," *Nature Medicine*, vol. 18, no. 7, pp. 1077–1086, 2012.

[17] S. Luo, Y. Liu, G. Liang et al., "The role of microRNA-1246 in the regulation of B cell activation and the pathogenesis of systemic lupus erythematosus," *Clinical Epigenetics*, vol. 7, p. 24, 2015.

[18] T. X. Lu, J. Hartner, E. J. Lim et al., "MicroRNA-21 limits in vivo immune response-mediated activation of the IL-12/IFN-gamma pathway, Th1 polarization, and the severity of delayed-type hypersensitivity," *Journal of Immunology*, vol. 187, no. 6, pp. 3362–3373, 2011.

[19] N. A. Stepicheva and J. L. Song, "Function and regulation of microRNA-31 in development and disease," *Molecular Reproduction and Development*, vol. 83, no. 8, pp. 654–674, 2016.

[20] M. M. Perry, S. A. Moschos, A. E. Williams, N. J. Shepherd, H. M. Larner-Svensson, and M. A. Lindsay, "Rapid changes in microRNA-146a expression negatively regulate the IL-1beta-induced inflammatory response in human lung alveolar epithelial cells," *Journal of Immunology*, vol. 180, no. 8, pp. 5689–5698, 2008.

[21] H. X. Fu, X. P. Fan, M. Li, M. J. Liu, and Q. L. Sun, "MiR-146a relieves kidney injury in mice with systemic lupus erythematosus through regulating NF-κB pathway," *European Review for Medical and Pharmacological Sciences*, vol. 23, no. 16, pp. 7024–7032, 2019.

[22] J. Zhang, Y. Cheng, W. Cui, M. Li, B. Li, and L. Guo, "MicroRNA-155 modulates Th1 and Th17 cell differentiation and is associated with multiple sclerosis and experimental autoimmune encephalomyelitis," *Journal of Neuroimmunology*, vol. 266, no. 1-2, pp. 56–63, 2014.

[23] G. Lerman, M. Sharon, R. Leibowitz-Amit, Y. Sidi, and D. Avni, "The crosstalk between IL-22 signaling and miR-197 in human keratinocytes," *PLoS One*, vol. 9, no. 9, article e107467, 2014.

[24] M. C. Hochberg, "Updating the American College of Rheumatology revised criteria for the classification of systemic lupus erythematosus," *Arthritis and Rheumatism*, vol. 40, no. 9, article 1725, 1997.

[25] J. Albrecht, L. Taylor, J. A. Berlin et al., "The CLASI (Cutaneous Lupus Erythematosus Disease Area and Severity Index): an outcome instrument for cutaneous lupus erythematosus," *The Journal of Investigative Dermatology*, vol. 125, no. 5, pp. 889–894, 2005.

[26] S. Méndez-Flores, G. Hernández-Molina, D. Azamar-Llamas, J. Zúñiga, J. Romero-Díaz, and J. Furuzawa-Carballeda, "Inflammatory chemokine profiles and their correlations with effector CD4 T cell and regulatory cell subpopulations in cutaneous lupus erythematosus," *Cytokine*, vol. 119, pp. 95–112, 2019.

[27] R. C. Lee, R. L. Feinbaum, and V. Ambros, "The C. elegans heterochronic gene *lin-4* encodes small RNAs with antisense complementarity to *lin-14*," *Cell*, vol. 75, no. 5, pp. 843–854, 1993.

[28] B. Wightman, I. Ha, and G. Ruvkun, "Posttranscriptional regulation of the heterochronic gene *lin-14* by *lin-4* mediates temporal pattern formation in C. elegans," *Cell*, vol. 75, no. 5, pp. 855–862, 1993.

[29] I. Alevizos and G. G. Illei, "MicroRNAs as biomarkers in rheumatic diseases," *Nature Reviews Rheumatology*, vol. 6, no. 7, pp. 391–398, 2010.

[30] C. Xiao, D. P. Calado, G. Galler et al., "MiR-150 controls B cell differentiation by targeting the transcription factor c-Myb," *Cell*, vol. 131, no. 1, pp. 146–159, 2007.

[31] N. A. Bezman, T. Chakraborty, T. Bender, and L. L. Lanier, "miR-150 regulates the development of NK and iNKT cells," *The Journal of Experimental Medicine*, vol. 208, no. 13, pp. 2717–2731, 2011.

[32] Y. Li, J. Su, F. Li, X. Chen, and G. Zhang, "MiR-150 regulates human keratinocyte proliferation in hypoxic conditions through targeting HIF-1α and VEGFA: implications for psoriasis treatment," *PLoS One*, vol. 12, no. 4, article e0175459, 2017.

[33] N. Honda, M. Jinnin, T. Kira-Etoh et al., "miR-150 down-regulation contributes to the constitutive type I collagen overexpression in scleroderma dermal fibroblasts via the induction of integrin β3," *The American Journal of Pathology*, vol. 182, no. 1, pp. 206–216, 2013.

[34] J. Q. Chen, G. Papp, P. Szodoray, and M. Zeher, "The role of microRNAs in the pathogenesis of autoimmune diseases," *Autoimmunity Reviews*, vol. 15, no. 12, pp. 1171–1180, 2016.

[35] W. Li, Y. F. Wu, R. H. Xu, H. Lu, C. Hu, and H. Qian, "miR-1246 releases RTKN2-dependent resistance to UVB-induced apoptosis in HaCaT cells," *Molecular and Cellular Biochemistry*, vol. 394, no. 1-2, pp. 299–306, 2014.

[36] M. Aksenenko, N. Palkina, A. Komina, L. Tashireva, and T. Ruksha, "Differences in microRNA expression between melanoma and healthy adjacent skin," *BMC Dermatology*, vol. 19, no. 1, p. 1, 2019.

[37] P. Xia, X. Fang, Z. H. Zhang et al., "Dysregulation of miRNA146a versus IRAK1 induces IL-17 persistence in the psoriatic skin lesions," *Immunology Letters*, vol. 148, no. 2, pp. 151–162, 2012.

[38] K. D. Taganov, M. P. Boldin, K. J. Chang, and D. Baltimore, "NF-κB-dependent induction of microRNA miR-146, an inhibitor targeted to signaling proteins of innate immune responses," *Proceedings of the National Academy of Sciences of the United States of America*, vol. 103, no. 33, pp. 12481–12486, 2006.

[39] L. Barbollat-Boutrand, N. Joly-Tonetti, M. Dos Santos et al., "MicroRNA-23b-3p regulates human keratinocyte differentiation through repression of TGIF1 and activation of the TGF-ß-SMAD2 signalling pathway," *Experimental Dermatology*, vol. 26, no. 1, pp. 51–57, 2017.

[40] A. Kraemer, I.-P. Chen, S. Henning et al., "UVA and UVB irradiation differentially regulate microRNA expression in human primary keratinocytes," *PLoS One*, vol. 8, no. 12, article e83392, 2013.

[41] H. Li, X. Han, K. Zuo et al., "miR-23b promotes cutaneous wound healing through inhibition of the inflammatory responses by targeting ASK1," *Acta Biochimica et Biophysica Sinica*, vol. 50, no. 11, pp. 1104–1113, 2018.

[42] K. S. Amr, F. S. Bayoumi, F. T. Elgengehy, S. O. Abdallah, H. H. Ahmed, and E. Eissa, "The role of microRNA-31 and microRNA-21 as regulatory biomarkers in the activation of T

lymphocytes of Egyptian lupus patients," *Rheumatology International*, vol. 36, no. 11, pp. 1617–1625, 2016.

[43] D. Di Girolamo, R. Ambrosio, M. A. De Stefano et al., "Reciprocal interplay between thyroid hormone and microRNA-21 regulates hedgehog pathway–driven skin tumorigenesis," *The Journal of Clinical Investigation*, vol. 126, no. 6, pp. 2308–2320, 2016.

[44] M. Zhou, X. Yu, Z. Jing, W. Wu, and C. Lu, "Overexpression of microRNA-21 inhibits the growth and metastasis of melanoma cells by targeting MKK3," *Molecular Medicine Reports*, vol. 20, no. 2, pp. 1797–1807, 2019.

[45] W. Fan, D. Liang, Y. Tang et al., "Identification of microRNA-31 as a novel regulator contributing to impaired interleukin-2 production in T cells from patients with systemic lupus erythematosus," *Arthritis and Rheumatism*, vol. 64, no. 11, pp. 3715–3725, 2012.

[46] D. Li, X. I. Li, A. Wang et al., "MicroRNA-31 promotes skin wound healing by enhancing keratinocyte proliferation and migration," *The Journal of Investigative Dermatology*, vol. 135, no. 6, pp. 1676–1685, 2015.

[47] B. Zhou, X. X. Zuo, Y. S. Li et al., "Integration of microRNA and mRNA expression profiles in the skin of systemic sclerosis patients," *Scientific Reports*, vol. 7, p. 42899, 2017.

[48] H. Zhu, Y. Li, S. Qu et al., "MicroRNA expression abnormalities in limited cutaneous scleroderma and diffuse cutaneous scleroderma," *Journal of Clinical Immunology*, vol. 32, no. 3, pp. 514–522, 2012.